

A Derivation of Aerosol Optical Depth Estimates from Direct Normal Irradiance Measurements

Yun Gon Lee¹⁾ · Chang Ki Kim^{2),3)*}

Received 14 February 2024 Revised 4 March 2024 Accepted 12 March 2024 Published online 18 March 2024

ABSTRACT This study introduces a method for estimating Aerosol Optical Depth (AOD) using Broadband Aerosol Optical Depth (BAOD) derived from direct normal irradiance and meteorological factors observed between 2016 and 2017. Through correlation analyses between BAOD and atmospheric components such as Rayleigh scattering, water vapor, and tropospheric nitrogen dioxide, significant relationships were identified, enabling accurate AOD estimation. The methodology demonstrated high correlation coefficients and low Root Mean Square Errors (RMSE) compared to actual AOD₅₀₀ measurements, indicating that the attenuation effects of water vapor and the direct impact of tropospheric nitrogen dioxide concentration are crucial for precise aerosol optical depth estimation. The application of BAOD for estimating AOD₅₀₀ across various time scales—hourly, daily, and monthly—showed the approach's robustness in understanding aerosol distributions and their optical properties, with a high coefficient of determination (0.96) for monthly average AOD₅₀₀ estimates. This study simplifies the aerosol monitoring process and enhances the accuracy and reliability of AOD estimations, offering valuable insights into aerosol research and its implications for climate modeling and air quality assessment. The findings underscore the viability of using BAOD as a surrogate for direct AOD₅₀₀ measurements, presenting a promising avenue for more accessible and accurate aerosol monitoring practices, crucial for improving our understanding of aerosol dynamics and their environmental impacts.

Key words Aerosol Optical Depth (AOD), Broadband Aerosol Optical Depth (BAOD), Direct normal irradiance, Meteorological observations, Correlation analysis

Nomenclature

T_{air} : transmittance of trace gases

T_{sol} : transmittance of aerosols

T_{gas} : transmittance of gaseous substance

θ : solar zenith angle

\AA : Ångstrom Exponent

m_{sol} : mass factor for aerosols

m_{air} : mass factor for Rayleigh scattering

m_{gas} : mass factor for gaseous substance

m_{w} : mass factor for water vapor

m_{nt} : mass factor for nitrogen dioxide

τ_{sol} : optical depth for aerosols

τ_{oz} : optical depth for ozone

τ_{gas} : optical depth for gaseous substance

τ_{w} : optical depth for precipitable water

τ_{nt} : optical depth for nitrogen dioxide

τ_{c} : optical depth for Rayleigh scattering

1) Associate Professor, Department of Astronomy and Space Sciences, Chungnam National University

2) Professor, Department of Energy Engineering, University of Science and Technology

3) Principal Researcher, Renewable Energy Big Data Laboratory, Korea Institute of Energy Research

*Corresponding author: cckim@kier.re.kr

Tel: +82-42-860-3517

Fax: +82-42-860-3462

Subscript

- AOD₅₀₀ : AOD observed at 500 nm
 DNI : direct normal irradiance
 AOD : aerosol optical depth
 BAOD : broadband aerosol optical depth

1. Introduction

With the recent increase in fine particulate matter, there has been a growing public interest in aerosols. Aerosols refer to solid particles suspended in the atmosphere, which generally scatter or absorb the solar radiation reaching the Earth's surface. The parameter that represents this effect is called the Aerosol Optical Depth (AOD), and monitoring AOD is important due to its spatial and temporal variability and its significant impact on climate change.^[1] The international program for AOD observation, AERONET (AERosol RObotic NETwork), began in the 1990s.^[2] However, AOD observations based on ground measurements face spatial limitations, which are supplemented by interpreting images monitored through satellites observing the Earth's atmosphere.^[3,4] Nonetheless, AOD estimation from satellite images also involves errors due to its reliance on indirect observation techniques.

On the other hand, observations of solar radiation or insolation have been conducted over long periods.^[5] Considering that aerosols are a major factor in the attenuation of insolation, techniques for estimating aerosol concentration through insolation analysis have been researched (e.g.,^[6~11]). In the initial study, Linke^[6] calculated turbidity or haziness using Broadband Direct Normal Irradiance, considering that turbidity is influenced not only by aerosols but also by water vapor and the solar zenith angle, making it unsuitable to consider only the effects of aerosols. Unsworth

and Monteith^[7] parameterized Broadband AOD as a function of the solar zenith angle and water vapor. More recently, Gueymard^[8] presented an algorithm for estimating Ångström turbidity β and Schüepf turbidity using a pyrhelimeter. Qiu^[10] also proposed a method for estimating AOD between 619 and 1575 nm from Direct Normal Irradiance. Gueymard^[12] showed that Broadband Direct Normal Irradiance is sensitive to changes in AOD and suggested that it could be used to estimate AOD. However, most studies have been limited to BAOD, which differs from AOD at 500 nm.

In South Korea, the AERONET program is in operation, with a sunphotometer installed at the Yonsei University Science Center to observe AOD at different wavelengths. Concurrently, the Korea Institute of Energy Research is conducting observations of horizontal global irradiance and Direct Normal Irradiance at Seoul National University. Therefore, this study aims to calculate BAOD using Direct Normal Irradiance observations and predict AOD at 500 nm using the correlation between BAOD and AOD observed through a sunphotometer. AOD at 500 nm is usually employed in atmospheric sciences because visible rays are between 400 and 700 nm, and then the other atmospheric components like Ozone do not affect the attenuation of solar irradiance.

2. Broadband Aerosol Optical Depth

The transmittance due to trace gases (T_{air}), aerosols (T_{sol}), and gaseous substances (T_{gas}) in the atmosphere for the solar spectrum is defined as in equation (1).

$$\begin{aligned}
 DNI &= DNI_o \times \prod_i^N T_i \\
 &= DNI_o \times (T_{air} \times T_{sol} \times T_{gas}) \\
 &= DNI_o \times \exp(-m_{air}\tau_{air} - m_{sol}\tau_{sol} - m_{gas}\tau_{gas}) \quad (1)
 \end{aligned}$$

Here, DNI represents the direct normal irradiance observed by a Pyrhelimeter, and DNI₀ is equivalent to the solar constant. Moreover, m_{sol} , m_{air} , m_{gas} represent the atmospheric mass factors for aerosols, Rayleigh scattering, and gaseous substances, respectively. Particularly, since atmospheric gaseous substances are classified into various types, it is necessary to detail them. Gueymard^[8] categorized atmospheric gaseous substances into water vapor (w), ozone (oz), stratospheric nitrogen dioxide (ns), tropospheric nitrogen dioxide (nt), and unspecified gaseous substances. Using equation (1), the optical depth for aerosols can be organized as in equation (2).

$$\tau_{sol} = \frac{1}{m_{sol}} \times \left[\ln \left(\frac{DNI_o}{DNI} \right) - (m_{air} \tau_{air} + m_{air} \tau_{oz} + m_{air} \tau_{ns} + m_w \tau_w + m_{nt} \tau_{nt}) \right] \quad (2)$$

In equation (2), assuming that the atmospheric mass factors for aerosols, water vapor, and tropospheric nitrogen dioxide are all the same, they can be expressed as a function of the solar zenith angle (θ), as presented by Gueymard and Vignola^[13] and Gueymard and Kambezidis.^[14]

$$m_{sol} = m_{air} = m_{nt} = \frac{1}{\cos \theta + 0.45665 \theta^{0.07} \times (96.4836 - \theta)^{-1.6970}} \quad (3)$$

$$m_w = \frac{1}{\cos \theta + 0.031141 \theta^{0.1} \times (92.4710 - \theta)^{-1.3814}} \quad (4)$$

For optical depths of trace gases other than aerosols, such as water vapor, the parameterization equations provided by Gueymard^[8] were used for calculations.

3. Research Data and Method

3.1 Data

3.1.1 Aerosol Optical Depth

Currently, AOD observations are being conducted on the rooftop of the Science Building at Yonsei University in Seoul through the AERONET (Aerosol Robotic NETwork) program. The data provided include AOD observed at 340, 380, 440, 500, 675, 870, 1020, 1640 nm, aerosol properties such as Ångstrom Exponent (Å) between 440 – 870 nm, 380 – 500 nm, 440 – 675 nm, 500 – 870 nm, 340 – 440 nm, and meteorological factors necessary for AOD estimation such as precipitable water, atmospheric mass factor, temperature, ozone, and nitrogen dioxide concentrations. The observation period has been ongoing from 2011 to the present, with a time resolution of 1 minute. As can be confirmed from the theoretical background, AOD is applicable only under clear sky conditions on clear days, hence there is no AOD data when sky is cloudy.

3.1.2 Direct Normal Irradiance

Direct solar irradiance, scattered irradiance, and global horizontal irradiance data observed from 2016 to 2018 for AOD estimation with a time resolution of 1 minute in Seoul National University. Although the AOD observation site and the direct solar irradiance observation site are both located in Seoul, there is a spatial difference between them. Considering that both sites have a time resolution of 1 minute for AOD and direct solar irradiance, a collocation process for the observation times is deemed necessary. Therefore, in this study, assuming clear sky conditions for AOD calculation, only data from clear sky conditions were used for direct solar irradiance observations. To verify clear sky conditions, the clear sky irradiance

calculation module of the UASIBS–KIER (University of Arizona Solar Irradiance Based on Satellite – Korea Institute of Energy Research) model developed by the Korea Institute of Energy Research was used, where ozone concentration, nitrogen dioxide concentration, and precipitable water were used as meteorological factors, directly inputting data provided by AERONET. Thus, clear sky irradiance was calculated for the same time periods when AOD is produced using the UASIBS–KIER model, and a clearness index was represented using clear sky irradiance and global horizontal irradiance as follows.

$$\text{Clearness Index} = \frac{\text{Global Horizontal Irradiance}}{\text{Clear Sky Irradiance}} \quad (5)$$

According to Kim *et al.* (2019),^[15] in a study analyzing clearness index by type, a clearness index greater than 0.9 generally indicates a cloudless sky, so this study also assumes clear conditions when the clearness index is greater than 0.9. Therefore, even if it is the same time period as when AOD was observed, if the clearness index at the direct solar irradiance observation site is less than 0.9, indicating the presence of clouds, it is difficult to theoretically estimate AOD, thus excluding it from the analysis. From 2016 to 2018, there were 71,208 AOD observations and 513,234 direct solar irradiance observations. After temporal collocation and clear sky classification for both sites, 50,425 data points were used in this study, including AOD, ozone concentration, nitrogen dioxide, precipitable water, and direct solar irradiance.

3.2 Methodology

As presented in Fig. 1, this study calculated BAOD using direct normal irradiance, precipitable water, ozone, and nitrogen dioxide concentrations observed

from 2016 to 2017, and developed a linear regression prediction model for AOD₅₀₀ through correlation analysis with AOD₅₀₀ observed at the AERONET site. This linear regression model was validated by comparing it with AOD₅₀₀ at the same site in 2018.

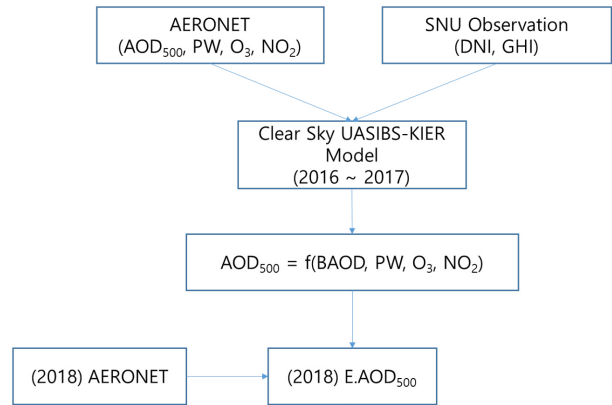


Fig. 1. Flowchart for research

4. Results and Discussions

To understand the correlation between direct normal irradiance and meteorological factors for the period 2016 to 2017, Fig. 2 shows the correlation between

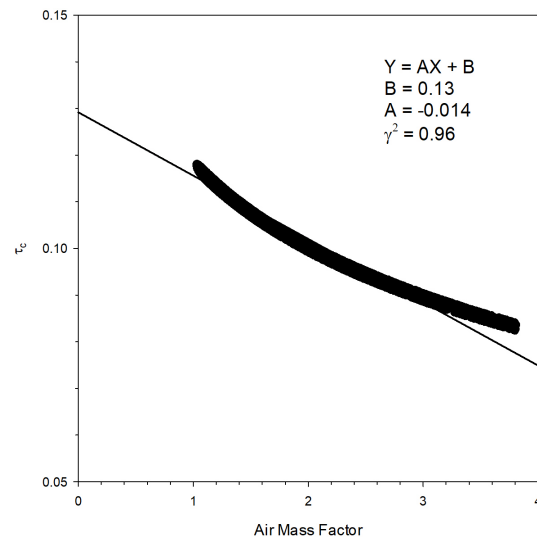


Fig. 2. Scatter plot of air mass factor and τ_c from 2016 to 2017 at Yonsei University

the atmospheric mass factor for Rayleigh scattering and τ_c , indicating an inverse relationship with the atmospheric mass factor. To analyze the attenuation effect due to water vapor, a scatter plot between precipitable water and τ_w is presented in Fig. 3. The coefficient of determination is 0.67, and the slope shows a positive value. The somewhat low coefficient of determination suggests that factors attenuating direct normal irradiance include not only precipitable water but also the atmospheric mass factor (solar zenith angle), which also affects the solar zenith angle. Lastly, Fig. 4, comparing tropospheric nitrogen dioxide concentration and its impact on τ_{nt} , shows that nitrogen dioxide optical depth is directly affected

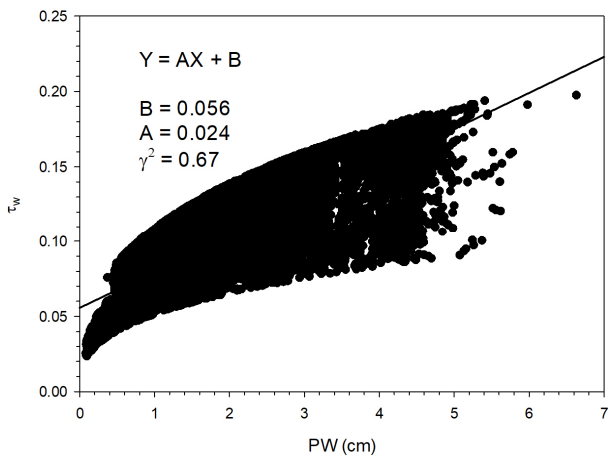


Fig. 3. Same as Fig. 2 except of precipitable water and τ_w

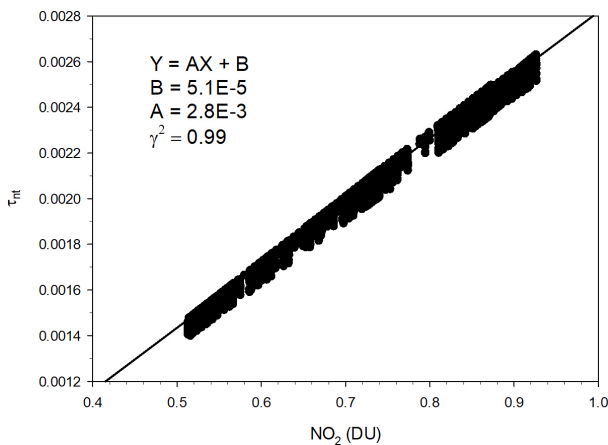


Fig. 4. Same as Fig. 2 except of NO_2 and τ_{nt}

by tropospheric nitrogen dioxide concentration, although its magnitude is smaller compared to other optical depths (τ_c and τ_w).

Using equation (2), (3), and (4), BAOD was calculated for the verification period (2016 to 2017). The relative frequency distribution of BAOD presented in Fig. 5 shows a Gamma distribution, with the highest frequency occurring between 0.06 and 0.10, accounting for 20% of the total datasets. The median of the overall distribution appears in the range where BAOD is 0.07 – 0.08, with about 50% occurring when it is less than 0.1.

Since the time resolution of direct normal irradiance is 1 minute, BAOD calculated using instantaneous direct normal irradiance was compared with AOD_{500} , and then BAOD and AOD_{500} were compared on an hourly, daily, and monthly basis by reducing the time resolution. The comparison between instantaneous BAOD and AOD_{500} in Fig. 6 shows a coefficient of determination of 0.70 and a slope of 1.2, indicating that AOD at 500 nm is generally about 20% larger than the broadband aerosol optical depth.

When comparing hourly BAOD and AOD_{500} , the coefficient of determination is similar, but the distribution of data decreases, which is due to the

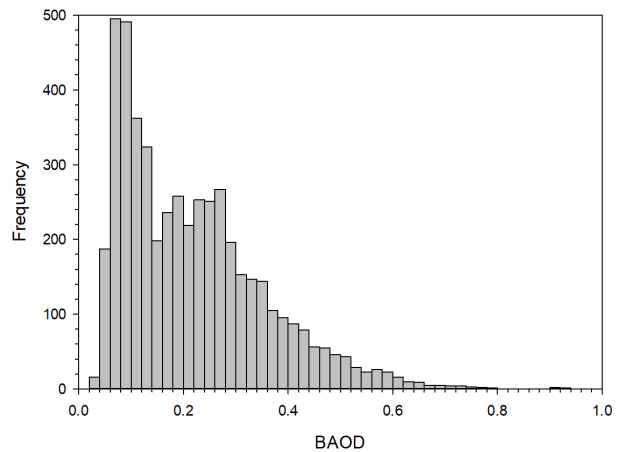


Fig. 5. Frequency of BAOD estimated by DNI observations at Seoul National University from 2016 to 2017

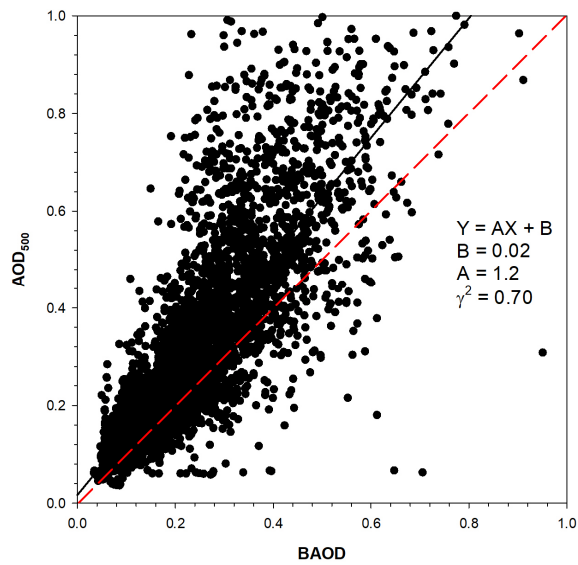


Fig. 6. Scatter plot of BAOD at Seoul National University and AOD₅₀₀ at Yonsei University at instantaneous time scale from 2016 to 2017

smoothing effect of averaging (not shown). Through these relationships, aerosol optical depth can be estimated with BAOD, defined as in equation (6).

$$\text{Hourly AOD}_{500} = 1.51 \times \text{BAOD} - 0.015 \quad (6)$$

BAOD obtained from direct normal irradiance observed in 2018 was calculated, and AOD₅₀₀ was estimated using equation (5), then compared with AOD₅₀₀ actually observed during this period. The coefficient of determination is 0.73, which translates to a correlation coefficient of about 0.85, indicating a relatively high correlation. The slope between the estimated and measured values is 0.74, suggesting that the estimates are lower than the measurements, indicating underestimation (Fig. 7). Therefore the estimation could be limited in a specific AOD range.

The correlation between daily average AOD₅₀₀ and BAOD observed from 2016 to 2017 was analyzed and presented in Fig. 8. Compared to the hourly comparison, the distribution of data is reduced, and the trend is clearer. Therefore, the coefficient of deter-

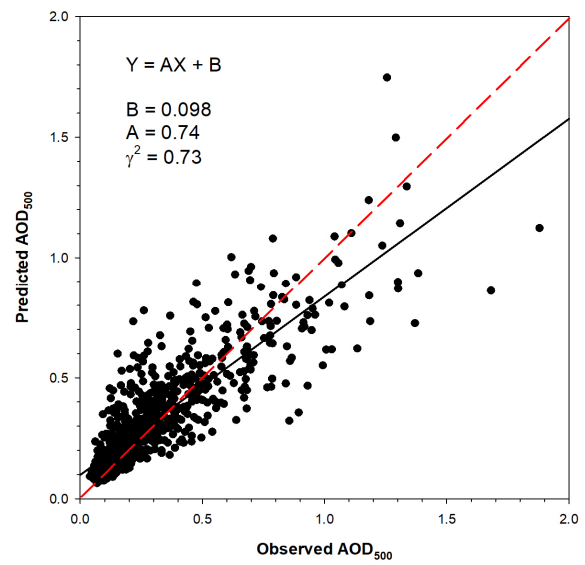


Fig. 7. Scatter plot of observed and predicted AOD₅₀₀ at hourly time scale in 2018

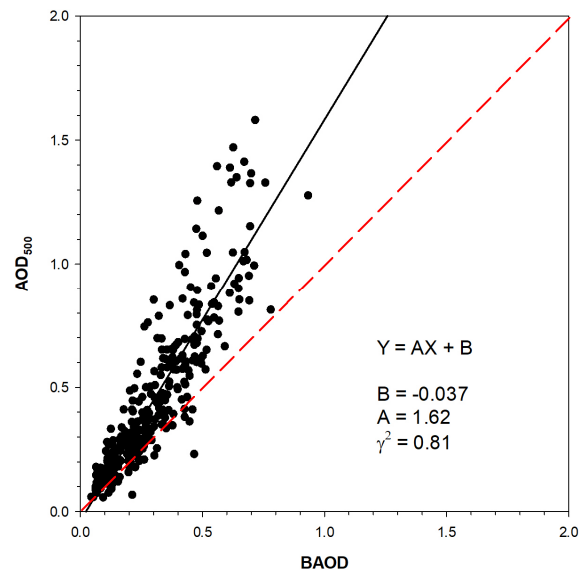


Fig. 8. Same as Fig. 6 except at daily time scale

mination is 0.81, and the correlation coefficient is 0.90, which is high. Through these relationships, daily AOD₅₀₀ was defined as follows:

$$\text{Daily AOD}_{500} = 1.62 \times \text{BAOD} - 0.037 \quad (7)$$

The comparison of measured AOD₅₀₀ in 2018 with the validation results is shown in Fig. 9. The coeffi-

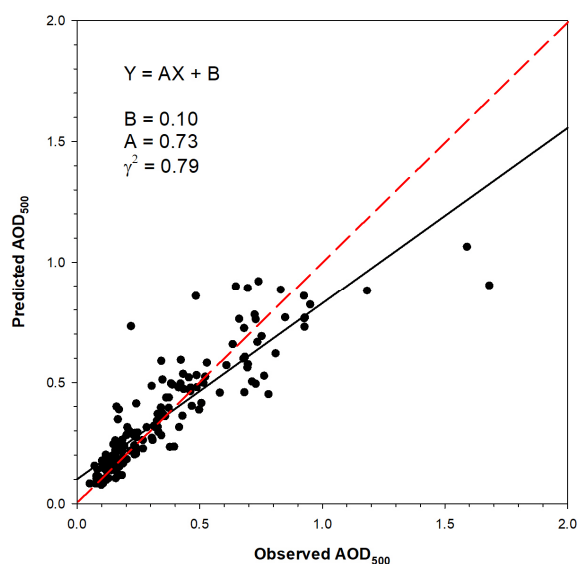


Fig. 9. Same as Fig. 7 except at daily time scale

coefficient of determination for the daily AOD₅₀₀ estimates increased to 0.79 compared to the hourly AOD₅₀₀ estimates. The daily AOD₅₀₀ estimates also show a tendency to underestimate compared to the measurements, maintaining consistency with the hourly AOD₅₀₀ estimates.

Lastly, to estimate monthly average AOD₅₀₀, BAOD was compared from 2016 to 2017. The coefficient of determination between the two physical quantities is 0.96, indicating that 96% of the explanatory power for AOD₅₀₀ can be attributed to BAOD, suggesting that BAOD can be used to estimate monthly average AOD₅₀₀ in the future. Equation (8) represents the linear correlation formula for monthly average AOD₅₀₀ based on BAOD.

$$\text{Monthly AOD}_{500} = 1.26 \times \text{BAOD} + 0.018 \quad (8)$$

Monthly average AOD₅₀₀ estimates were compared with monthly average AOD₅₀₀ observed in 2018 (Fig. 10). The Root Mean Square Error (RMSE) of the estimates against the measurements is about 0.038, indicating high reliability of AOD₅₀₀ estimated with BAOD, along with daily AOD₅₀₀.

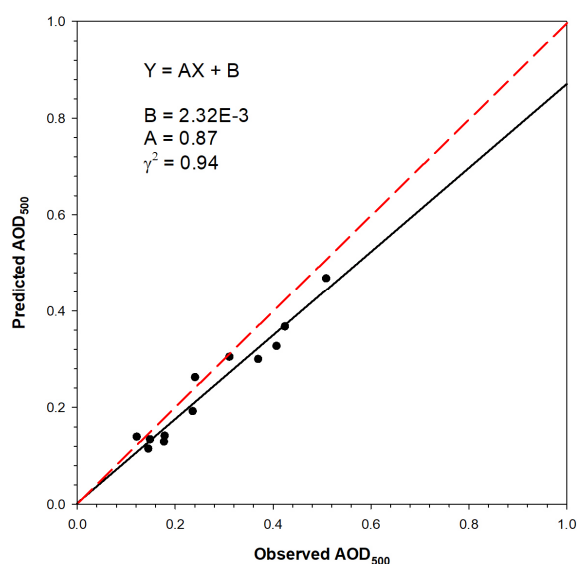


Fig. 10. Same as Fig. 7 except at monthly time scale

Table 1. Summary of root mean square error between observation and estimations for AOD₅₀₀ at hourly, daily and monthly time scale

| | Estimates | Reference |
|---------------------------------|-----------|-------------------------------|
| Hourly Mean AOD ₅₀₀ | 0.134 | 0.153 ~ 0.179 ^[16] |
| Daily Mean AOD ₅₀₀ | 0.130 | 0.132 ~ 0.315 ^[17] |
| Monthly Mean AOD ₅₀₀ | 0.038 | |

Table 1 summarizes the RMSE between the estimates and measurements of hourly, daily, and monthly average AOD₅₀₀, showing that AOD₅₀₀ derived from BAOD is more accurate compared to the RMSE range of AOD₅₀₀ estimates from satellite images.

5. Conclusions

In this study, we have demonstrated a method for estimating Aerosol Optical Depth (AOD) using Broad-band Aerosol Optical Depth (BAOD) derived from direct normal irradiance and meteorological factors observed between 2016 and 2017. Through detailed correlation analyses between BAOD and atmospheric

components such as Rayleigh scattering, water vapor, and tropospheric nitrogen dioxide, we found significant relationships that are crucial for accurate AOD estimation. The results show that BAOD can reliably estimate AOD₅₀₀, with the methodology exhibiting high correlation coefficients and low Root Mean Square Errors (RMSE) when compared to actual AOD₅₀₀ measurements. This suggests that the attenuation effects of water vapor and the direct impact of tropospheric nitrogen dioxide concentration are key factors in the precise estimation of aerosol optical depth.

Furthermore, the application of BAOD for estimating AOD₅₀₀ across various time scales—hourly, daily, and monthly—highlights the robustness of this approach in understanding aerosol distributions and their optical properties. The high coefficient of determination (0.96) for monthly average AOD₅₀₀ estimates emphasizes the potential of BAOD as a predictive tool for aerosol optical depth. This study not only simplifies the aerosol monitoring process but also enhances the accuracy and reliability of AOD estimations, contributing valuable insights into aerosol research and its implications for soiling impact in Photovoltaic system. The advancement presented in this study underscores the viability of using BAOD as a surrogate for direct AOD₅₀₀ measurements, offering a promising avenue for more accessible and accurate aerosol monitoring practices, which is crucial for improving our understanding of aerosol dynamics and their environmental impacts.

Acknowledgment

This work was supported by the Korea Institute of Energy Technology Evaluation and Planning (KETEP) grant funded by the Korea government (MOTIE) (2019371010006B, Development of core stabilizing technology for renewable power management system).

References

- [1] Seinfeld, J.H., and Pandis, S.N., 2016, “Atmospheric chemistry and physics: From air pollution to climate change”, 3rd Edition, John Wiley & Sons, New Jersey.
- [2] Holben, B.N., Eck, T.F., Slutsker, I., Tanré, D., Buis, J.P., Setzer, A., Vermote, E., Reagan, J.A., Kaufman, Y.J., and Nakajima, T., *et al.*, 1998, “AERONET—A federated instrument network and data archive for aerosol characterization”, *Remote Sensing of Environment*, **66**(1), 1-16.
- [3] Ruiz-Arias, J.A., Dudhia, J., Gueymard, C.A. and Pozo-Vázquez, D., 2013, “Assessment of the level-3 MODIS daily aerosol optical depth in the context of surface solar radiation and numerical weather modeling”, *Atmos. Chem. Phys.*, **13**(2), 675-692.
- [4] Antuña-Marrero, J.C., Cachorro Revilla, V., García Parrado, F., de Frutos Baraja, Á., Rodríguez Vega, A., Mateos, D., Estevan Arredondo, R. and Toledano, C., 2018, “Comparison of aerosol optical depth from satellite (MODIS), sun photometer and broadband pyrhelimeter ground-based observations in Cuba”, *Atmos. Meas. Tech.*, **11** (4), 2279-2293.
- [5] Stothers, R.B., 1996, “The great dry fog of 1783”, *Climatic Change*, **32**(1), 79-89.
- [6] Linke, F., 1922, “Transmission coefficient and turbidity factor”, *J Beitrage Phys Fr Atom*, **10** (2), 91-103.
- [7] Unsworth, M.H. and Monteith, J.L., 1972, “Aerosol and solar radiation in Britain”, *Quarterly Journal of the Royal Meteorological Society*, **98**(418), 778-797.
- [8] Gueymard, C.A., 1998, “Turbidity determination from broadband irradiance measurements: A detailed multi-coefficient approach”, *J. Appl. Meteorol.*, **37**(4), 414-435.
- [9] Qiu, J., 1998, “A method to determine atmospheric aerosol optical depth using total direct solar radiation”, *J Atmos Sci*, **55**(5), 744-757.
- [10] Qiu, J., 2001, “Broadband extinction method to determine atmospheric aerosol optical properties”, *Tellus B: Chemical and Physical Meteorology*, **53**(1), 72-82.
- [11] Qiu, J., 2003, “Broadband extinction method to determine aerosol optical depth from accumulated direct solar

- radiation”, *J. Appl. Meteorol.*, **42**(11), 1611-1625.
- [12] Gueymard, C.A., 2012, “Temporal variability in direct and global irradiance at various time scales as affected by aerosols”, *Solar Energy*, **86**(12), 3544-3553.
- [13] Gueymard, C. and Vignola, F., 1998, “Determination of atmospheric turbidity from the diffuse-beam broadband irradiance ratio”, *Solar Energy*, **63**(3), 135-146.
- [14] Gueymard, C. and Kambezidis, H.D., 1997, “Illuminance turbidity parameters and atmospheric extinction in the visible spectrum”, *Quarterly Journal of the Royal Meteorological Society*, **123**(539), 679-697.
- [15] Kim, C.K., Kim, H.G., Kang, Y.H., and Yun, C.Y., 2019, “Analysis of clear sky index defined by various ways using solar resource map based on Chollian satellite imagery”, *J Korean Solar Energy*, **39**(3), 47-57.
- [16] Lee, S., Choi, M., Kim, J., Kim, M., and Lim H., 2017, “Retrieval of aerosol optical depth with high spatial resolution using GOCI data”, *Korean Journal of Remote Sensing*, **33**(6), 961-970.
- [17] Lim, H., Choi, M., Kim, M., Kim, J., Go, S., and Lee, S., 2018, “Intercomparing the aerosol optical depth using the geostationary satellite sensors (AHI, GOCI and MI) from Yonsei AEROSOL Retrieval (YAER) algorithm”, *Journal of the Korean Earth Science Society*, **39**(2), 119-130.